Brain Struct Funct (2016) 221:1–20
DOI 10.1007/s00429-014-0888-4

ORIGINAL ARTICLE

Local corticotropin releasing hormone (CRH) signals to its receptor CRHR1 during postnatal development of the mouse olfactory bulb

Isabella Garcia · Paramjit K. Bhullar · Burak Tepe · Joshua Ortiz-Guzman · Longwen Huang · Alexander M. Herman · Lesley Chaboub · Benjamin Deneen · Nicholas J. Justice · Benjamin R. Arenkiel

Received: 25 February 2014 / Accepted: 9 September 2014 / Published online: 16 September 2014

Abstract Neuropeptides play important physiological functions during distinct behaviors such as arousal, learning, memory, and reproduction. However, the role of local, extrahypothalamic neuropeptide signaling in shaping synapse formation and neuronal plasticity in the brain is not well understood. Here, we characterize the spatiotemporal expression profile of the neuropeptide corticotropin-releasing hormone (CRH) and its receptor CRHR1 in the mouse OB throughout development. We found that CRH-expressing interneurons are present in the external plexiform layer, that its cognate receptor is expressed by granule cells, and show that both CRH and CRHR1 expression enriches in the postnatal period when olfaction becomes important towards olfactory-related behaviors. Further, we provide electrophysiological evidence that CRHR1-expressing granule cells functionally respond to CRH ligand, and that the physiological circuitry of CRHR1 knockout mice is abnormal, leading to impaired olfactory behaviors. Together, these data suggest a physiologically relevant role for local CRH signaling towards shaping the neuronal circuitry within the mouse OB.

Keywords Neuropeptide · CRH · CRF · Olfactory · Granule cell · GPCR · EPL · CRHR1 · CRFR1

I. Garcia · B. Tepe · J. Ortiz-Guzman · A. M. Herman · L. Chaboub · B. Deneen · B. R. Arenkiel
Program in Developmental Biology, Baylor College of Medicine, Houston, TX 77030, USA

I. Garcia
Medical Scientist Training Program, Baylor College of Medicine, Houston, TX 77030, USA

P. K. Bhullar · B. R. Arenkiel (✉)
Department of Molecular and Human Genetics, Baylor College of Medicine, Houston, TX 77030, USA
e-mail: arenkiel@bcm.edu

L. Huang · B. Deneen · B. R. Arenkiel
Department of Neuroscience, Baylor College of Medicine, Houston, TX 77030, USA

B. Deneen · B. R. Arenkiel
The Jan and Dan Duncan Neurological Research Institute at Texas Children's Hospital, Houston, TX 77030, USA

N. J. Justice
Institute of Molecular Medicine, University of Texas Health Science Center at Houston, Houston, TX 77030, USA

Introduction

Patterns of connectivity and communication between the diverse repertoires of neurons that make up the brain underlie complex behavior, physiological states, and allow for perception of environmental stimuli. Traditionally, hypothalamic neuropeptides, such as corticotropin-releasing hormone (CRH), somatostatin, oxytocin, neuropeptide Y, and vasopressin have been shown to be important for both brain development and function, where they influence physiological states such as arousal, stress, and reproduction (Bayatti et al. 2003; Chaves et al. 2013; Holzer et al. 2012; Merrill et al. 2013; Ramirez-Sanchez et al. 2013; Vale et al. 1981, 1983). Due to the vascularity of the hypothalamus, secreted neuropeptides can have long-ranging effects in distant brain regions that harbor cells that express cognate receptors (Bayatti et al. 2003; Inutsuka and Yamanaka 2013a, b; Iovino et al. 2012; Zwanzger et al. 2012). Depending on the brain region, neuropeptides function either as neurotransmitters, or act via slower neuromodulatory mechanisms (Maras and Baram 2012; Roozendaal et al. 2002; Schmolesky et al. 2007).

Additionally, neuropeptides have been implicated in dendritic outgrowth and neuroprotection (Chen et al. 2004; Hanstein et al. 2008; Sheng et al. 2012). Given the important roles of neuromodulators and neuropeptides towards regulating neuronal function, we sought to investigate possible roles that neuropeptides play towards shaping synapse development and plasticity, and/or remodeling of both existing and *de novo* brain circuits.

Extrahypothalamic neuropeptidergic interneurons have been identified throughout the brain (Le Magueresse and Monyer 2013; Ma et al. 2006; Rudy et al. 2011; Xu et al. 2013). However, neuropeptide expression patterns have largely served as a classification scheme, leaving the precise neuropeptidergic signaling mechanisms poorly understood. Because neuropeptides selectively bind specific neuropeptide receptors, it is important to identify the detailed local expression patterns of extrahypothalamic neuropeptides and their cognate receptors, with the larger goal of dissecting the precise physiological functions of neuropeptide signaling within distinct brain regions.

Extrahypothalamic brain regions with prominent neuropeptide signaling include the hippocampus (Maras and Baram 2012) and the olfactory system (Huang et al. 2013; Lepousez et al. 2010a, b), two regions of the mouse brain where continuous neurogenesis, apoptosis, synaptogenesis, and circuit integration occur throughout life (Abrous et al. 2005; Ming and Song 2005). To determine if local neuropeptide signaling plays a role in brain regions that exhibit high neuronal plasticity and turnover both during development and into adulthood, we examined the mouse olfactory system.

The mouse olfactory system is an ideal model to investigate mechanisms of neuronal maturation, synaptogenesis, and circuit integration because of its well-described feature of sustained neurogenesis throughout life (Abrous et al. 2005; Alvarez-Buylla and Garcia-Verdugo 2002; Ming and Song 2005). In the olfactory system, new neurons are continuously generated in the subventricular zone (Alvarez-Buylla and Garcia-Verdugo 2002; Ming and Song 2011) and migrate via the rostral migratory stream to populate the olfactory bulb (OB), where a majority become inhibitory granule cells (Gheusi et al. 2013; Lledo and Saghatelyan 2005). Granule cells extend their dendritic arbors into the external plexiform layer (EPL) where they form dendrodendritic connections with principal mitral and tufted cells (Chen et al. 2000; Isaacson and Strowbridge 1998; Schoppa et al. 1998). This connectivity plays a prominent role in shaping olfaction (Abraham et al. 2010; Belnoue et al. 2011; Breton-Provencher et al. 2009; Mouret et al. 2009).

Interestingly, granule cell circuit integration is an activity-dependent process (Arenkiel et al. 2011; Kelsch et al. 2009; Yamaguchi and Mori 2005). Throughout later stages of neuronal migration and synaptogenesis, granule cells receive numerous synaptic and extrasynaptic inputs that convey activity-dependent cues that help guide the integration of these new neurons into the pre-established OB circuitry (Arenkiel et al. 2011; Eyre et al. 2008; Pressler and Strowbridge 2006). Neuromodulators and neuropeptides are important candidates for shaping this process, and are thus likely to play important roles towards neuronal plasticity and circuit integration.

We have recently identified a select population of EPL interneurons with high expression levels of the neuropeptide CRH, and have shown that these neurons form GABAergic connections with mitral cells (Huang et al. 2013). However, the role of CRH-mediated signaling by EPL interneurons within the OB has not been investigated. Hypothalamic CRH is implicated in mediating stress responses, arousal, and reproduction by acting on two CRH receptors, CRHR1 and CRHR2 (Perrin et al. 1993, 1995). In the central nervous system, CRHR1 is expressed at higher levels than its counterpart CRHR2 (Allen Brain Atlas), and CRH shows a higher binding affinity to CRHR1 (Bale and Vale 2004). CRHR1 is a 7-transmembrane domain G_s-coupled receptor, and its activation triggers signaling cascades that affect diverse physiological functions, depending on the cell type in which it is expressed (Berger et al. 2006; Blank et al. 2003; Perrin et al. 1993; Thiel and Cibelli 1999). Given the heterogeneous cell population of the OB, and that CRH is only expressed in a select subset of OB interneurons, we hypothesized that local cells express CRHR1, providing a potential neuromodulatory signaling mechanism for CRH within the OB circuitry.

Here, we describe the detailed spatiotemporal expression profile of CRH ligand in a restricted population of OB EPL interneurons, and further show that its cognate receptor CRHR1 is dynamically expressed in granule cells that are continually generated throughout life. This spatiotemporally restricted CRH neuropeptide-receptor match first appears in the early postnatal period, and is sustained throughout adulthood. Further, we provide evidence that CRHR1-expressing granule cells physiologically respond to CRH ligand, and mice that lack CRHR1 exhibit impaired OB circuit function and olfactory behaviors. Together, our data reveal a novel, locally acting, and physiologically relevant interaction between two different interneuron subpopulations with important roles in shaping the OB circuitry and behavioral outputs.

Materials and methods

Animals

All experimental animals were treated in compliance with the United States Department of Health and Human

Services and the Baylor College of Medicine IACUC guidelines. Mice were reared on 12-h light–dark cycles with access to food and water ad libitum. *Crh-Cre knock-in* (Taniguchi et al. 2011), *Rosa*$^{lsl\text{-}tdTomato}$ *knock-in* (Arenkiel et al. 2011), *Crhr1-EGFP BAC transgenic* (Justice et al. 2008) and *Crhr1*$^{-/-}$ (Smith et al. 1998) mice were previously described. *Crh-Cre*$^{+/-}$; *Rosa*$^{lsl\text{-}tdTom/+}$ mice were obtained by crossing male *Crh-Cre*$^{+/-}$ to female *Rosa*$^{lsl\text{-}tdTom/lsl\text{-}tdTom}$ mice. Embryonic tissues were obtained from embryos of timed-pregnant females at E16.5 and E18.5. Presence of plugs was assumed to be embryonic day 0.5. Mice were genotyped using standard polymerase chain reaction from isolated tail DNA.

Immunohistochemistry

To characterize the expression of CRH and CRHR1 in the OB, mice were deeply anesthetized using isoflurane, and perfused intracardially with phosphate-buffered saline (PBS) and 4 % paraformaldehyde (PFA). Brains were dissected and postfixed in 4 % PFA/PBS overnight at 4 °C. The next day, fixed brains were transferred to fresh PBS, and 50-µm free-floating OB slices were cut using a Compresstome (Precisionary Instruments, San Jose, CA) (Selever et al. 2011). Confocal microscopy was performed using a Leica TCS SPE confocal microscope under a 10 or 20× objective. For immunohistochemistry, free-floating tissue sections were incubated in blocking solution (10 % normal goat serum, 0.3 % Triton-X in PBS, pH 7.35) for 1 h at room temperature. OB tissue sections were stained overnight at 4 °C using the following primary antibodies diluted in blocking solution: guinea pig anti-Parvalbumin (1:500, Synaptic Systems 195004, Germany), mouse anti-GABA (1:2,000, Millipore MAB316, Billerica MA), rabbit anti-Calretinin (1:1,000, Millipore MAB377, Billerica MA), rabbit anti-VGlut1 (1:500, Synaptic Systems 135302, Germany), rabbit anti-TBX21 (1:500, gift from Dr. Sachiko Mitsui, RIKEN Brain Science Institute, Japan), rabbit anti-Tyrosine Hydroxylase (1:2,000, Millipore AB152, Billerica MA), and rabbit anti-Calbindin (1:500, Abcam AB9481, Cambridge MA). The following day, OB tissue sections were washed 4 × 15 min in phosphate-buffered saline with 0.1 % Triton-X (PBST). Secondary Alexa-633 anti-rabbit, mouse or guinea pig (Invitrogen, Carlsbad, CA) were diluted 1:500 in blocking solution and applied for 1 h at room temperature. Sections were washed 4 × 15 min in PBST as above and mounted using Vectashield mounting medium (Vector Laboratories, Burlingame, CA). Tissue sections stained with secondary antibodies only served as negative antibody controls.

CRHR1 and CRHR2 expression analysis

For CRHR1 and CRHR2 mRNA transcript analysis, OBs (~24 mg tissue per animal) from wild-type mice were dissected out, placed in 1-ml Trizol reagent (Ambion, Invitrogen, Carlsbad, CA), and homogenized using a 1.5-ml presterilized pestle. Samples were allowed to incubate at room temperature for 5 min, followed by addition of 0.2 ml of chloroform. The sample was again incubated at room temperature for 2 min and centrifuged at 12,000× *g* for 15 min at 4 °C. The upper aqueous phase was pipetted into a new tube, 0.5 ml of isopropanol was added, and the mixture was incubated at room temperature for 10 min. The tube was centrifuged at 12,000× *g* for 10 min at 4 °C, and the supernatant was removed. The RNA pellet was washed with 1 ml of 75 % ethanol, vortexed, and centrifuged at 7,500× *g* for 5 min at room temperature. The pellet was air-dried for 15 min and resuspended in 40-µl RNase-free water at 60 °C. RNA was DNAse-digested using the manufacturer's protocol (Promega). DNAse was inactivated via phenol–chloroform extraction, and purified RNA was quantified using a NanoDrop (Wilmington, DE). First-strand cDNA was synthesized using the High Capacity cDNA Reverse Transcription Kit (Applied Biosystems). Negative controls did not contain reverse transcriptase. Transcripts were amplified using standard PCR conditions (95 °C for 120 s, 95 °C for 20 s, 60 °C for 20 s, 72 °C for 20 s, 40 cycles, 72 °C for -300 s, 4 °C for ∞). Primer sequences were as follows: GAPDH F-tgatgacatcaagaaggtggtgaag R-tccttggaggccatgtaggccat, CRHR1 F-ccaggatcagcagtgtgaga R-agtggcccaggtagttgatg, CRHR2 F-ctggaacctcatcaccacct R-gtccaccaaatcaccagctt.

Nonradioactive double in situ hybridization

The expression of CRHR1 and EGFP was analyzed in OB sections from *Crhr1-EGFP* transgenic mice using a robotic platform as previously described (Yaylaoglu et al. 2005). The published protocol was modified to allow the visualization of two probes simultaneously using a combination of digoxigenin (DIG)- and fluorescein (FITC)-labeled riboprobes and development of signal by fluorescently labeled tyramide. All modifications described were performed at room temperature, and the abbreviated solutions are described in detail in the original protocol. In brief, the protocol changes were: DIG- and FITC-labeled probes were added and hybridized simultaneously. Following the previously described hybridization, stringency washes, blocking and anti-DIG-horseradish peroxidase (HRP) steps, the DIG-labeled probes were developed by the

addition of tyramide-Cy3 (Tyramide Plus Cy3, Perkin Elmer) according the manufacturer's protocol. The slides were then washed in (Tris–HCl–NaCl with Tween 20 (TNT), treated with 0.2 M HCl for 30 min to quench any remaining HRP activity, washed in TNT, and incubated in TNB-blocking solution for 15 min prior to incubation in anti-FITC-HRP antibody (1/500, Roche) for 30 min. After washing in TNT, the slides were treated with tyramide-FITC (Tyramide Plus FITC, Perkin Elmer) according to the manufacturer's protocol to develop the signal from the FITC-labeled probe. Slides were then washed in TNT and mounted in Vectashield with DAPI (Vector Labs).

Cell type-specific birthdating

For cellular birthdating of CRH+ EPL interneurons, timed-pregnant females at E16.5 and E18.5 from *Crh-Cre*$^{+/-}$; *ROSA*$^{\text{lsl-tdTom/+}}$ crosses, or P0, P7, P14, and P30 animals received one dose of EdU intraperitoneally (Invitrogen, Carlsbad CA, 50 mg/kg) and were killed 30 days post injection. 14-μm OB sections were made throughout the olfactory bulb (from Bregma: 3.92 to 4.28 mm), and every 5th section was processed as described in the EdU Click-It reaction kit (Invitrogen, Carlsbad, CA), and imaged under a 20× objective, zoom factor 3, 10-μm *Z*-stack. The ratio of EdU/tdTom double-positive EPL interneurons (region of 180 × 180 × 10 μm^3) was divided by the number of tdTom-positive cells to obtain the percentage of EPL interneurons born at the time of injection ($n = 3$ mice per time period, 6 OBs, 5 slices per bulb, 5 sections per slice). For birthdating of CRHR1+ cells in the granule cell layer, pregnant *Crhr1-EGFP* mice at E16.5 and E18.5, or P0, P7, P14, P30, P90, and P180 mice were pulsed with EdU. 14-μm OB sections were collected as above, and the ratio of EdU/EGFP double-positive granule cells (180 × 180 × 10 μm^3) was divided by the number of EGFP-positive cells to obtain the percentage of CRHR1+ granule cells born at the time of injection ($n = 3$ mice per time period, 6 OBs, 5 slices per bulb, 5 sections per slice). Statistical analysis was performed using ANOVA and Graphpad software.

Imaging and mean fluorescent intensity analysis

All images were taken using a Leica TCS SPE confocal microscope under a 10 or 20× objective with a *Z* depth spanning 10–12 μm. To determine the mean fluorescent intensity of *Crhr1-EGFP* mice at different time points, OB layer-specific images were taken under a 20× objective with a digital zoom factor of 3. Intensity measurements were performed using ImageJ software from five layer-specific sections per slice, five slices per animal, from three animals per time period.

Electrophysiology

Coronal OB slices (300 μm) were prepared from *Crhr1-EGFP* or *Crhr1*$^{+/+}$ and *Crhr1* $^{-/-}$mice (P21-P35). Animals were deeply anesthetized using isoflurane, and perfused intracardially with ice-cold artificial cerebrospinal fluid (aCSF, in mM: 122 NaCl, 3 KCl, 1.2 NaH_2PO_4, 26 $NaHCO_3$, 20 glucose, 2 $CaCl_2$, 1 $MgCl_2$, 305–315 mOsm, pH 7.3). Brains were dissected and rapidly embedded in low melting point agarose, sectioned into ice-cold oxygenated (5 % CO_2, 95 % O_2) dissection buffer (in mM: 87 NaCl, 2.5 KCl, 1.6 NaH_2PO_4, 25 $NaHCO_3$, 75 sucrose, 10 glucose, 1.3 ascorbic acid, 0.5 $CaCl_2$, 7 $MgCl_2$), recovered (15 min at 37 °C) in oxygenated ACSF, and acclimated at room temperature for 10 min prior to electrophysiological recordings. Borosilicate glass electrodes (Sutter Instruments, Novato CA) were used for whole cell patch-clamp recordings. Electrodes were pulled with a tip resistance between 4 and 7 MΩ, and filled with internal solution (in mM: 110 $CsMeSO_3$, 0.2 EGTA, 4 NaCl, 30 HEPES, 2 Mg-ATP, 0.3 Na-GTP,14 creatine phosphate). During recordings, coronal OB slices were placed in a room temperature chamber mounted on an Olympus upright microscope (BX50WI) and perfused with oxygenated ACSF. Cells were visualized under differential interference contrast imaging. Data were obtained via a Multiclamp 700B amplifier, low-pass Bessel filtered at 4 kHz, and digitized on computer disk (Clampex, Axon Instruments). CRH (500 nM) was bath-applied to the recording chamber of *Crhr1-EGFP* slices, and spontaneous excitatory/inhibitory post-synaptic currents (EPSCs or IPSCs) were measured before and 5 min after CRH application. Neurons were held at − 80 mV for EPSC recordings or at 0 mV for IPSC recordings. Statistical analyses were performed using Student's *t* test.

Odor detection threshold

Control *Crhr1* $^{+/+}$($n = 5$) and experimental *Crhr1*$^{-/-}$ ($n = 5$) mice were habituated to experimental conditions for 4 consecutive days. Habituation involved placing mice in a clean 35 cm × 17 cm × 12.5 cm cage and exposing them to two mineral oil-soaked cotton-tipped applicators, suspended from opposite ends of the cage lid, for 5 min. During the testing phase of this experiment, one of the mineral oil-soaked cotton-tipped applicators was replaced with a cotton-tipped applicator soaked in a 1×10^{-6} dilution (in mineral oil) of an odorant. Six odorants were presented [(+)terpinen-4-ol, 2-heptanol, butyraldehyde, 1-octanol, isoamyl acetate, and limonene (−), obtained from Sigma, St. Louis MO], with only two odorants tested per day. New cages and cotton-tipped applicators were used for every odorant. Sniffing time for the mineral oil

versus odorant was recorded during the course of a 10-min trial for each odorant presented that day. Mice were subsequently tested at 1×10^{-5}, 1×10^{-4}, and 1×10^{-3} dilutions of each odorant using the same procedures. An odor detection index (sniffing time for odor/total sniffing time) was calculated for each mouse, at every concentration of every odorant. Odor indexes of control and experimental mice were analyzed via repeated ANOVA measures in SPSS, in which four and six levels were assigned to the within-subjects factors of concentration and odorant, respectively.

Odor discrimination

Control *Crhr1*$^{+/+}$ ($n = 8$) and experimental *Crhr1*$^{-/-}$ ($n = 8$) mice, previously habituated to experimental conditions, were placed in a clean 35 cm × 17 cm × 12.5 cm cage, in which a cotton-tipped applicator soaked in a 1×10^{-3} dilution of butyraldehyde was suspended from the cage lid. Sniffing time for the butyraldehyde was measured during three 10-min habituation trials, with a 5-min delay between trials. 5 min following habituation, mice were placed in a cage in which two cotton-tipped applicators, one soaked in butyraldehyde and the other in isoamyl acetate (1×10^{-3} in mineral oil), were suspended from opposite ends of the cage lid. Sniffing time for the familiar (butyraldehyde) versus novel (isoamyl acetate) odorant was recorded during the course of a 10-min trial. The following day, this test was repeated with another set of odorants, 2-heptanol and limonene (−). All odorants were obtained from Sigma, St. Louis MO. For each set of odorants, comparisons between control and Crhr1$^{-/-}$ were made using a Student's *t* test.

Olfactory short-term memory

Crhr1$^{+/+}$ ($n = 8$) and *Crhr1*$^{-/-}$ ($n = 8$) mice, previously habituated to experimental conditions, were placed in a clean 35 cm × 17 cm × 12.5 cm cage, in which a cotton-tipped applicator soaked in a 1×10^{-3} dilution (in mineral oil) of (+) terpinen-4-ol was suspended from the cage lid. Sniffing time for the (+) terpinen-4-ol applicator was recorded during a 10-min trial, after which mice were returned to their home cages. Following a 30-min delay, mice were again placed in the experimental cage, where a cotton-tipped applicator freshly soaked in the same odorant was inserted into the same position in the cage lid. Time spent sniffing the applicator was recorded during a 10-min trial. During the subsequent 3 days, delay times of 60, 90, and 120 min were tested using a different odorant each day [limonene (−), 1-octanol, and isoamyl acetate]. Within *Crhr1*$^{+/+}$ and *Crhr1*$^{-/-}$ groups, sniffing time during the first and second exposures of odorants were compared using Student's *t* tests.

Results

CRH expression is initiated postnatally in EPL interneurons

The mouse OB contains diverse populations of interneurons that differ morphologically and functionally. Granule cells make up the vast majority of interneurons in the OB and have been extensively studied (Gheusi et al. 2013; Isaacson and Strowbridge 1998; Lledo and Saghatelyan 2005). However, EPL interneurons have recently received attention due to their roles in shaping the olfactory bulb circuitry (Hamilton et al. 2005; Huang et al. 2013; Kato et al. 2013; Miyamichi et al. 2013), and have been classified as Parvalbumin-expressing (PV+), fast-spiking GABAergic interneurons (Batista-Brito et al. 2008; Hamilton et al. 2005; Huang et al. 2013; Kato et al. 2013; Kosaka and Kosaka 2008). We have recently discovered that a subpopulation of EPL interneurons expresses the neuropeptide CRH, in addition to GABA (Huang et al. 2013). Given the role of neuropeptides in physiological homeostasis and synaptic plasticity, we questioned if local CRH signaling by EPL interneurons plays additional roles within the OB circuitry.

To first determine the spatiotemporal expression profile of CRH during development, we crossed *Crh-Cre* mice to conditional tdTomato reporter mice to obtain *Crh-Cre*$^{+/-}$; *Rosa*$^{\text{LSL-TdTom/+}}$ mice (Fig. 1). We analyzed these animals at E16.5, E18.5, and P0 and did not observe CRH expression at these time points in the OB (data not shown). Bulbar CRH expression first appeared at postnatal day 7 (P7), and increased substantially from P7 to P30 (Fig. 1b). Because CRH is expressed in a select population of interneurons throughout the cortex as well as in the paraventricular nucleus of the hypothalamus, we validated our reporter allele via expression of CRH in these domains (Fig. 1c, d).

Given that EPL interneurons make up a subpopulation of PV+ interneurons in the OB (Hamilton et al. 2005; Huang et al. 2013; Kato et al. 2013; Kosaka and Kosaka 2008), we sought to determine if the temporally controlled expression pattern of CRH correlated with expression of mature neuronal identity markers. Immunohistochemistry against PV revealed an expression pattern that mirrored CRH, with very low expression in the early postnatal period, and increased expression levels from P14 into adulthood (Fig. 2a, b). At P60, 95 % of CRH+ EPL interneurons were also PV+. Interestingly, this value varied from our previous quantification of PV expression (Huang et al. 2013), where we initially reported that 81.5 % of CRH+ EPL interneurons also expressed PV at weaning age (P21). This differential result suggests that

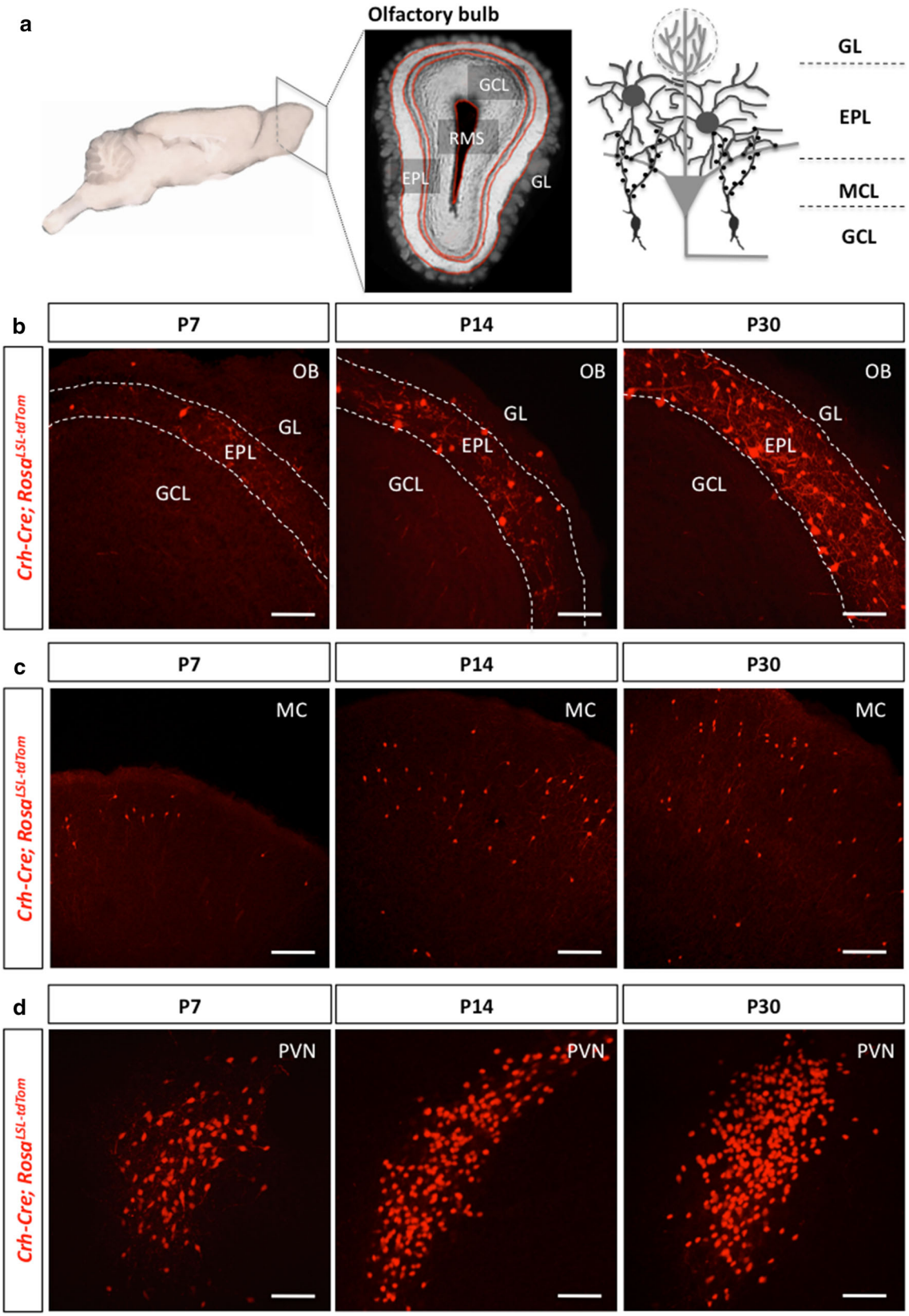
a
Olfactory bulb
GCL
RMS
EPL
GL
GL
EPL
MCL
GCL
b
P7
P14
P30
Crh-Cre; Rosa^LSL-tdTom
OB
GL
EPL
GCL
c
MC
d
PVN

◀**Fig. 1** CRH expression in olfactory bulb EPL interneurons is initiated during the postnatal period. **a** Simplified schematic of the olfactory bulb circuitry (*RMS* rostral migratory stream, *GCL* granule cell layer, *EPL* external plexiform layer, *MCL* mitral cell layer, *GL* glomerular layer). Confocal image of the expression pattern of *Crh-Cre*; *Rosa*$^{lsl\text{-}tdTomato/+}$ mice at P7, P14, and P30 in the (**b**) olfactory bulb (*scale bar* 100 μm), the **c** motor cortex (MC) (*scale bar* 150 μm), and the **d** hypothalamic paraventricular nucleus (PVN) (*scale bar* 100 μm)

CRH and PV expression in EPL interneurons is likely not stabilized until early adulthood.

Since EPL interneurons have been previously shown to be GABAergic (Hamilton et al. 2005; Huang et al. 2013; Kato et al. 2013; Kosaka and Kosaka 2008; Miyamichi et al. 2013), we next set out to determine if the expression pattern of CRH correlated with the onset of expression of the neurotransmitter GABA in the EPL. We found that once EPL interneurons expressed CRH, they also expressed GABA; and this occurred as early as P14 (Fig. 2c). Interestingly, CRH+ EPL interneurons comprise a rare subset of mature neuronal subtypes, apart from cerebellar Purkinje cells, mitral cells, and retinal photoreceptor cells (Mullen et al. 1992) with relatively weak expression of the neuronal marker NeuN (Fig. 2d, e). However, nearly all CRH+ EPL interneurons expressed the calcium-binding protein Calretinin (Fig. 2f, g).

It has been previously shown that different interneuron populations in the OB are generated during different developmental stages. EPL interneurons are predominantly generated postnatally, and are not replaced in adulthood (Batista-Brito et al. 2008). Because EPL interneurons did not express CRH until the postnatal period, we next set out to establish the birthdate of these cells during development. For this, we pulsed *Crh-Cre*$^{+/-}$; *Rosa*$^{\text{LSL-TdTom/+}}$ mice with the proliferation marker EdU at multiple time points to determine the percentage of CRH+ EPL interneurons that are generated at different stages of development between E16.5 and P30 (Fig. 2h, i). We found that CRH+ EPL interneurons are continuously generated during the early postnatal life, with a large increase in cell proliferation between P7 and P14 (Fig. 2i). These findings were consistent with a previous report of the birthdating of EPL interneurons within the OB (Batista-Brito et al. 2008). Taken together, these data suggest that CRH+ EPL interneurons are predominantly generated postnatally, and soon thereafter express markers of mature neuronal identity.

CRHR1 gradually enriches postnatally and into adulthood

Because the physiological effects of CRH are mediated by binding to one of the two CRH receptors, CRHR1 and CRHR2 (Perrin et al. 1993, 1995), we next examined the receptor expression within the OB. Expression analysis of cDNA from wild-type OB tissue revealed that CRHR1 transcript is expressed at higher levels than CRHR2, consistent with in situ hybridization data reported in the Allen Brain Atlas (Fig. 3a).

In order to determine the precise cellular identity and spatiotemporal pattern of CRHR1 expression within the OB, we utilized a BAC transgenic *Crhr1-EGFP* allele that allows dynamic visualization of CRHR1 expression throughout the brain (Justice et al. 2008). We validated its expression profile by double in situ hybridization against EGFP and CRHR1, and found that it recapitulates endogenous CRHR1 expression (Fig. 3b). Using this mouse allele, we observed that CRHR1 expression is low during the embryonic period, but gradually enriches postnatally both in the granule cell layer (GCL) and glomerular layer (GL) (Fig. 4). Interestingly, between P7 and P14, CRHR1+ granule cells become enriched in the very outer regions of the granule cell layer (GCL), closely juxtaposing mitral cells (Fig. 4a). In contrast, between P14 and P30, the inner regions of the GCL are populated with CRHR1+ cells. Throughout development, there is no expression of CRHR1 in the core of the OB.

Because CRHR1 is strongly expressed in the outer GCL that directly juxtaposes the mitral cell layer (Fig. 4), we questioned if CRHR1 is also expressed by mitral cells. Immunohistochemistry against the mitral cell-specific marker TBX-21 (Mitsui et al. 2011) and the vesicular glutamate transporter VGlut1 showed that CRHR1 expression is completely absent in mitral cells of the OB (Fig. 5).

Given that a subpopulation of CRHR1+ cells within the OB is located in the glomerular layer (Figs. 4, 5), we next sought to determine the identity of these neurons. We found that 26 ± 7 % of CRHR1+ periglomerular cells expressed Tyrosine Hydroxylase (TH), suggesting that a subpopulation of these cells are dopaminergic (Fig. 6a). However, none of the CRHR1+ periglomerular cells expressed either of the calcium-binding proteins Calbindin (CB) or Calretinin (CR) (Fig. 6b, c). Additionally, we found that TH, CB, and CR are mutually exclusive within the GL of the OB (Fig. 6d–f).

Because CRHR1 is strongly expressed within the GCL, and granule cells in the OB are continuously generated throughout life (Gheusi et al. 2013; Lledo and Saghatelyan 2005), we set out to (1) investigate if CRHR1-expression in granule cells correlates with expression of markers of mature neuronal identity, and (2) determine when during development CRHR1+ granule cells are predominantly generated. To address the first question, we asked if CRHR1 is expressed in mature granule cells. Towards this, we performed immunohistochemistry against NeuN and CR from P0 until P30 (Fig. 7a–d). We found that granule

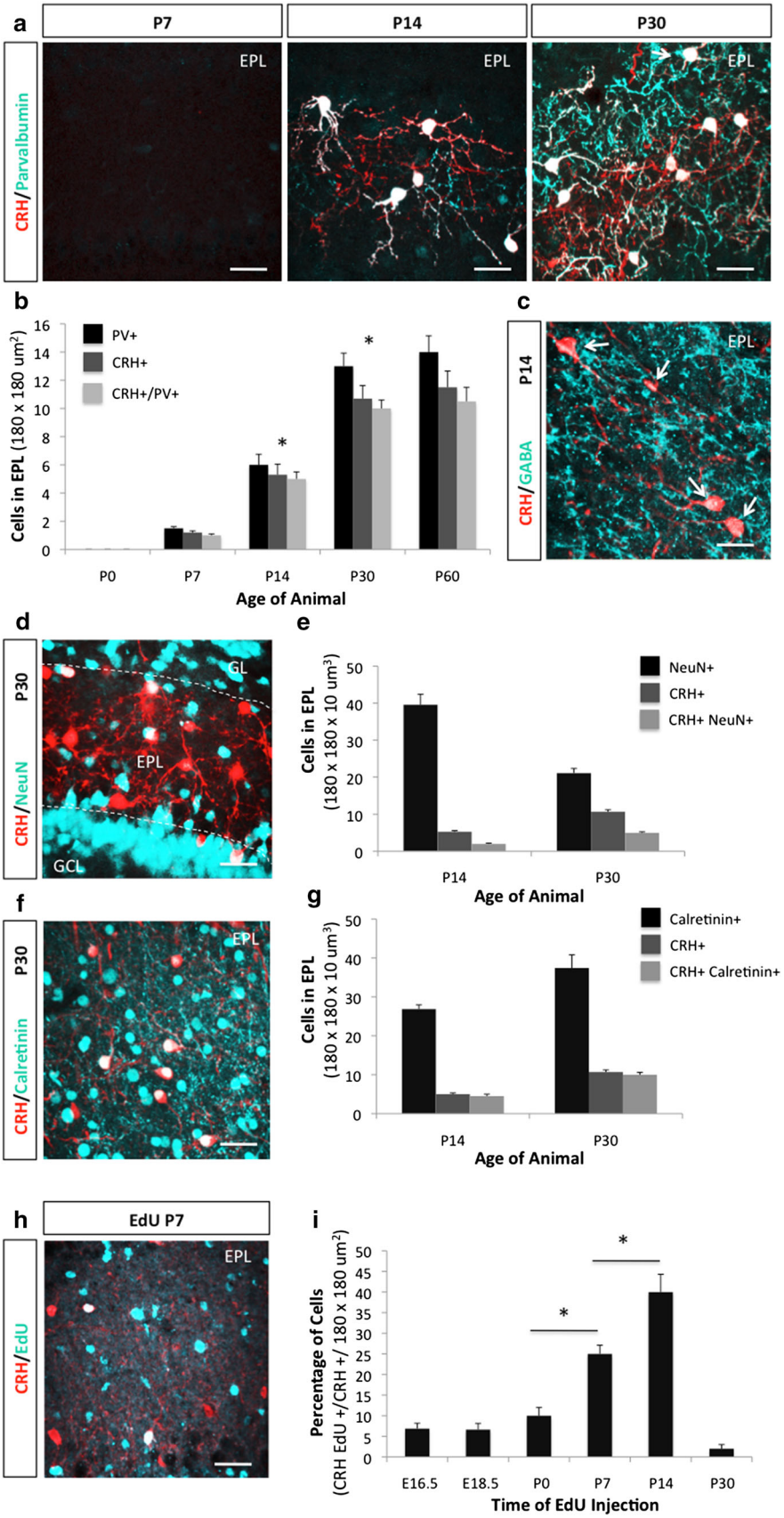

Fig. 2 CRH+ EPL interneurons are predominantly generated postnatally. **a** Expression pattern of *Crh-Cre*; *Rosa*$^{lsl\text{-}tdTomato/+}$ mice at P7, P14, and P30 co-stained with the interneuron marker Parvalbumin (*scale bar* 30 μm). **b** Quantification of the expression of Parvalbumin and CRH+ interneurons in the EPL between P0 and P60. Confocal immunohistochemistry image of **c** GABA on *Crh-Cre*; *Rosa*$^{lsl\text{-}tdTomato/+}$ EPL tissue at P14 (*scale bar* 20 μm), and **d** NeuN at P30 (*scale bar* 30 μm). **e** Quantification of the expression of NeuN and CRH+ interneurons at P14 and P30. **f** Confocal image of Calretinin in CRH+ EPL interneurons at P30 (*scale bar* 40 μm). **g** Quantification of the expression of Calretinin and CRH+ interneurons at P14 and P30. **h** Example confocal image of EdU expression in CRH+ neurons pulsed at P7 (*scale bar* 40 μm). **i** Quantification of the percentage of CRH+ EPL interneurons born between E16.5 and P30 (*$p < 0.05$). All data points represent averages ± SEM

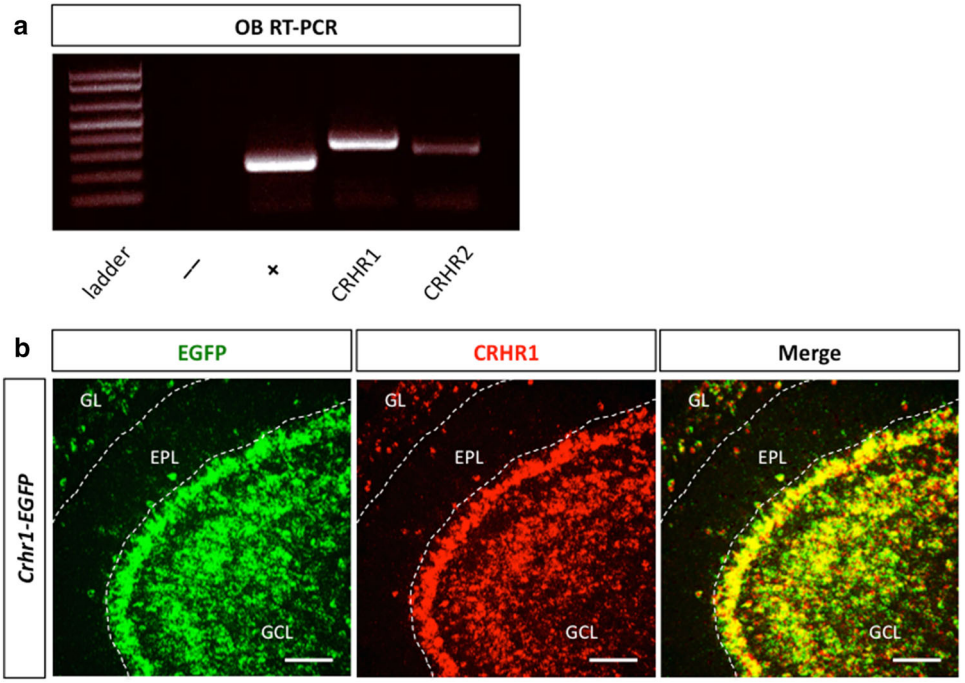

Fig. 3 The CRH receptor CRHR1 is enriched in the olfactory bulb. **a** Semi-quantitative RT-PCR of olfactory bulb cDNA amplifying CRHR1 and CRHR2 mRNA transcript (−ctrl RNA without reverse transcriptase,+ctrl GAPDH). **b** Double in situ hybridization image of EGFP and CRHR1 expression in *Crhr1-EGFP* BAC transgenic olfactory bulb slice (*GCL* granule cell layer, *EPL* external plexiform layer, *GL* glomerular layer, *scale bar* 200 μm)

cells that express CRHR1 are also NeuN and CR+. In fact, CRHR1+ granule cells comprise a subset of NeuN+, CR+ interneurons within the OB.

With this in mind, we next wished to determine when during development CRHR1+ granule cells are generated, and secondarily, when the highest proportion of CRHR1+ granule cells appears. To answer this question, we pulsed *Crhr1-EGFP* transgenic mice with the proliferation marker EdU between embryonic days E16.5 and P180, and assayed for EdU and CRHR1-double marker expression in the GCL (Fig. 7e, f). We found that CRHR1+ granule cells are continuously generated throughout life, beginning from the late embryonic period and continuing into adulthood. Interestingly, the highest proportion of CRHR1+ granule cells is generated postnatally, which coincides with when CRH+ EPL interneurons first appear within the OB (Figs. 1, 2).

CRH signaling influences olfactory bulb circuitry, function, and olfactory performance

Given that CRH and CRHR1+ interneurons show spatially restricted distribution within the OB, we next wondered if these two cell populations are juxtaposed anatomically, and performed a double-reporter, 3-allele lineage analysis of *Crh-Cre*; *Rosa*$^{lsl\text{-}tdTom}$; *Crhr1-EGFP* mice (Fig. 8). We found that CRHR1 is strongly expressed by granule cells (Figs. 4, 7, 8), whose dendritic arbors extend into the EPL and precisely juxtapose CRH+ EPL interneurons (Fig. 8).

CRH is a neuropeptide that can act both as a neurotransmitter and neuromodulator. Thus, we next sought to investigate the role of CRH on CRHR1+ granule cells. For this, we performed electrophysiological recordings of CRHR1+ granule cells before and after bath application of CRH ligand (Fig. 9a, b) and found that CRH bath application did not elicit rapid changes in membrane potential, nor fast synaptic responses in CRHR1+ granule cells (data not shown). Together, these data suggested that CRH does not act as a bona fide neurotransmitter onto granule cells, but may rather instead function as a neuromodulator. In support of this, indeed we observed gradual, selective, and time-dependent decreases in the amplitudes of excitatory postsynaptic currents (EPSCs) without affecting their frequencies (Fig. 8c, d). Furthermore, CRH ligand did not cause any changes in rise and decay time of neuronal firing (Fig. 9e, f).

Because CRH acts by binding to CRHR1, and CRHR1 is a G-protein-coupled receptor, we wondered if removing CRHR1 from granule cells would cause changes in the electrophysiological properties of the OB circuitry. Towards this, we utilized *Crhr1*$^{-/-}$ mice (Smith et al. 1998) and recorded EPSCs from granule cells and inhibitory postsynaptic currents (IPSCs) from mitral cells (Fig. 10a–d). We found that granule cells from *Crhr1*$^{-/-}$ mice showed significantly higher EPSC frequencies than control granule cells (Fig. 10d). To next test the effect of removing CRHR1 from granule cells onto mitral cells, we recorded IPSCs from mitral cells and found significantly decreased amplitudes and frequencies (Fig. 10g, h), supporting decreased inhibitory drive from granule cells onto mitral cells. Together these data suggest that granule cells

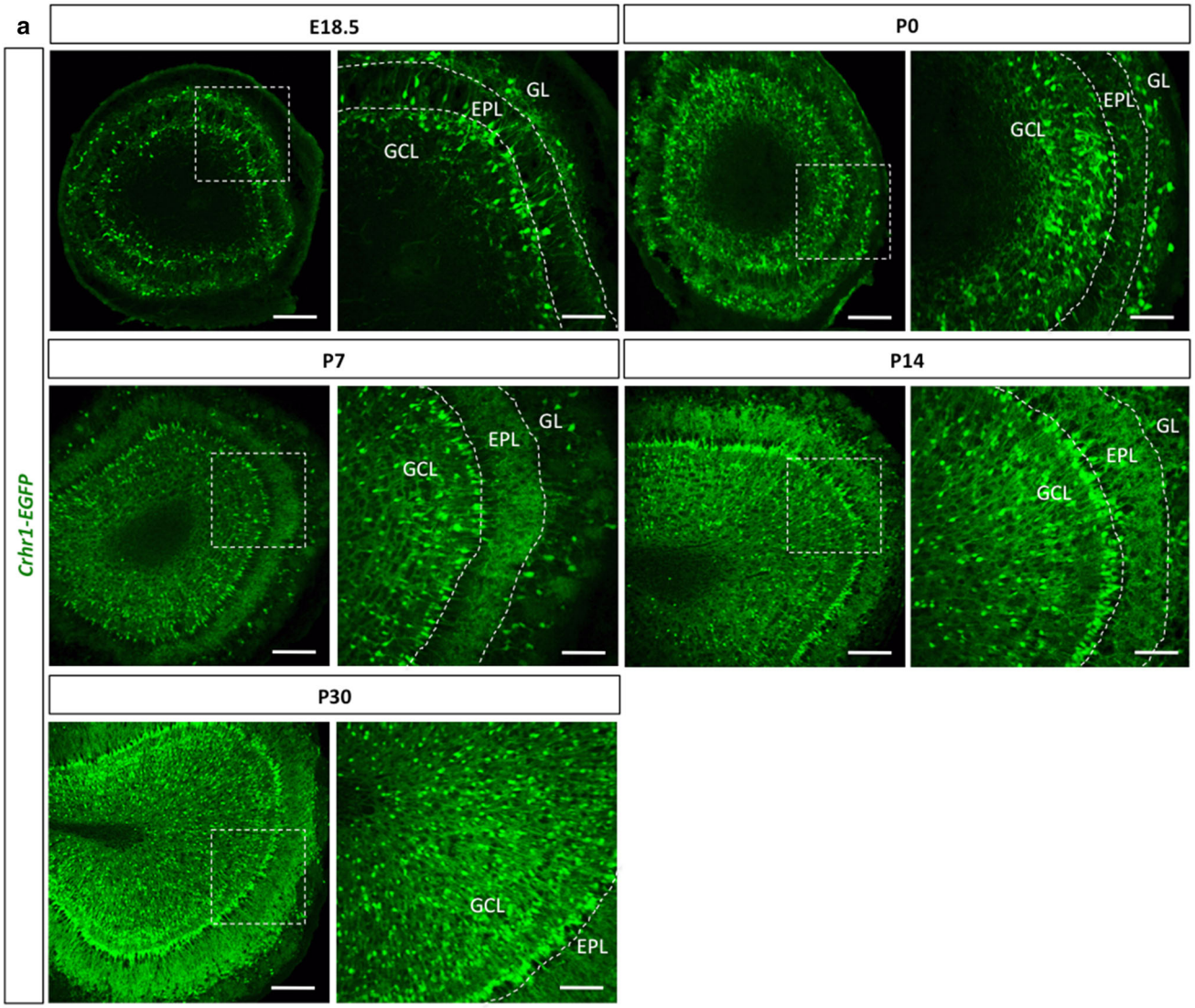
a
E18.5
P0
P7
P14
P30
Crhr1-EGFP
GL
EPL
GCL

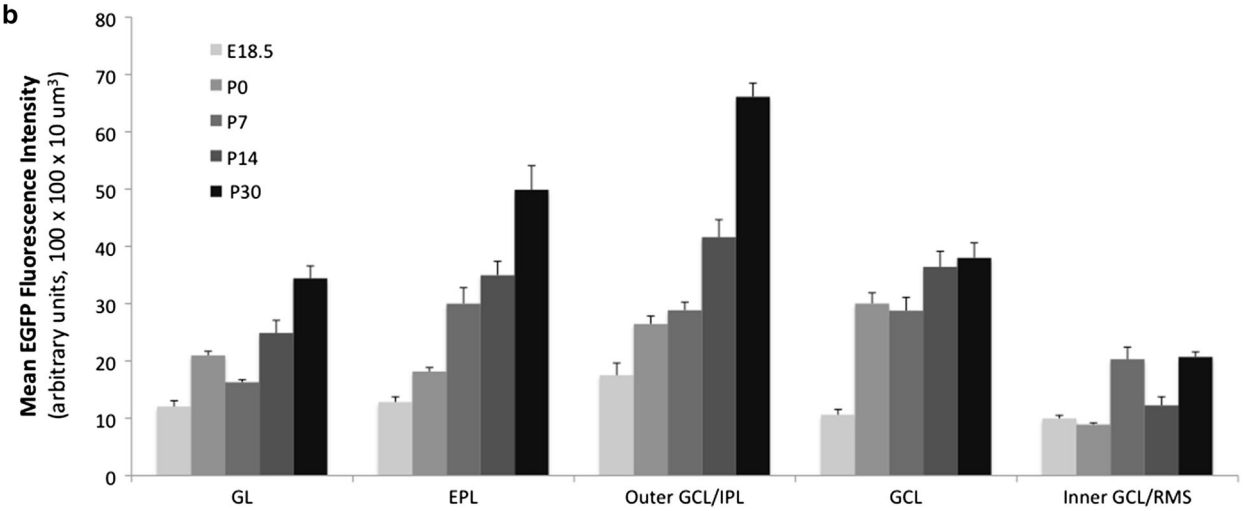
b
Mean EGFP Fluorescence Intensity
(arbitrary units, 100 x 100 x 10 um³)
E18.5
P0
P7
P14
P30
0
10
20
30
40
50
60
70
80
GL
EPL
Outer GCL/IPL
GCL
Inner GCL/RMS

◀**Fig. 4** Olfactory bulb CRHR1 expression enriches postnatally and into adulthood. **a** Olfactory bulb expression pattern of *Crhr1-EGFP* transgenic mice throughout development at E18.5, P0, P7, P14, and P30 (*GL* glomerular layer, *EPL* external plexiform layer, *GCL* granule cell layer, *scale bar* 300 and 100 μm for inserts, respectively). **b** Quantification of the layer-specific expression pattern of *Crhr1-EGFP* transgenic mice between E18.5 and P30. All data points represent averages ± SEM

in $Crhr1^{-/-}$ mice receive more excitatory currents from mitral cells, but are unable to inhibit mitral cells at normal levels. This decreased level of inhibition, in turn, could explain the higher frequency of EPSCs onto granule cells due to their dendrodendritic connectivity.

Granule cells form inhibitory synapses onto mitral cells and have a prominent role in shaping olfactory output to higher cortical regions (Isaacson and Strowbridge 1998; Luo and Katz 2001). Moreover, it has been described that dysfunctional granule cells lead to impaired olfactory behaviors and olfactory memory (Breton-Provencher et al. 2009; Gheusi et al. 2000). Having determined that the mitral cell–granule cell interaction is abnormal in $Crhr1^{-/-}$ mice, we wanted to determine if CRH signaling plays a role in olfactory behavior. Using $Crhr1^{-/-}$ mice, we first evaluated odor detection responses, and found that $Crhr1^{-/-}$ mice showed normal detection of several odorants across various concentrations (Fig. 10i), suggesting no obvious deficit in olfactory sensory neurons. Interestingly however, despite normal odor detection, these mice exhibited impaired ability to discriminate a novel from a habituated odorant (Fig. 10j). This phenotype was independent of the odorants presented, as two separate groups of odorants validated these data. With the proposed role of granule cells in olfactory memory (Breton-Provencher et al. 2009; Lazarini et al. 2009; Rochefort et al. 2002), we next tested $Crhr1^{-/-}$ animals on short-term (non-operant) olfactory memory tasks, which do not require discrimination between odorants. $Crhr1^{-/-}$ mice showed deficits in short-term olfactory memory compared to controls (Fig. 10k). Together with electrophysiological data, our behavior assays suggest that CRHR1-mediated signaling plays an important role in shaping the olfactory circuitry, and ultimately, olfactory behavior.

Discussion

Here, we have characterized the dynamic expression patterns of CRH and CRHR1 in the OB over time, and have shown that this interaction is important for the proper functioning of the OB circuitry. Interestingly, CRHR1 expression in the OB appears prior to CRH, and is first observed embryonically. CRHR1 expression then significantly increases in the postnatal period, coincident with CRH (Fig. 11). Because olfaction is refined during this time period, the expression of CRH and CRHR1 in distinct interneuron subtypes of the OB suggests that local CRH signaling may serve physiologically important roles towards olfactory processing, synaptic function, and/or

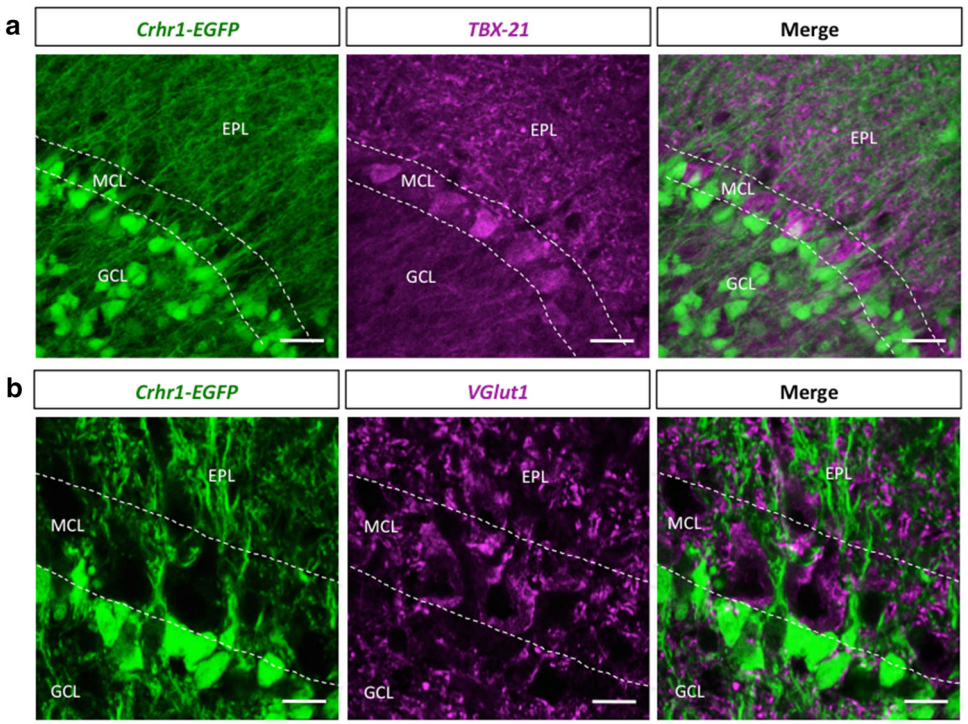

Fig. 5 CRHR1 is not expressed by olfactory bulb mitral cells. Immunohistochemistry confocal image of *Crhr1-EGFP* olfactory bulb tissue stained with **a** TBX-21 (*GCL* granule cell layer, *MCL* mitral cell layer, *EPL* external plexiform layer, *scale bar* 50 μm), and **b** VGlut1 (*scale bar* 20 μm)

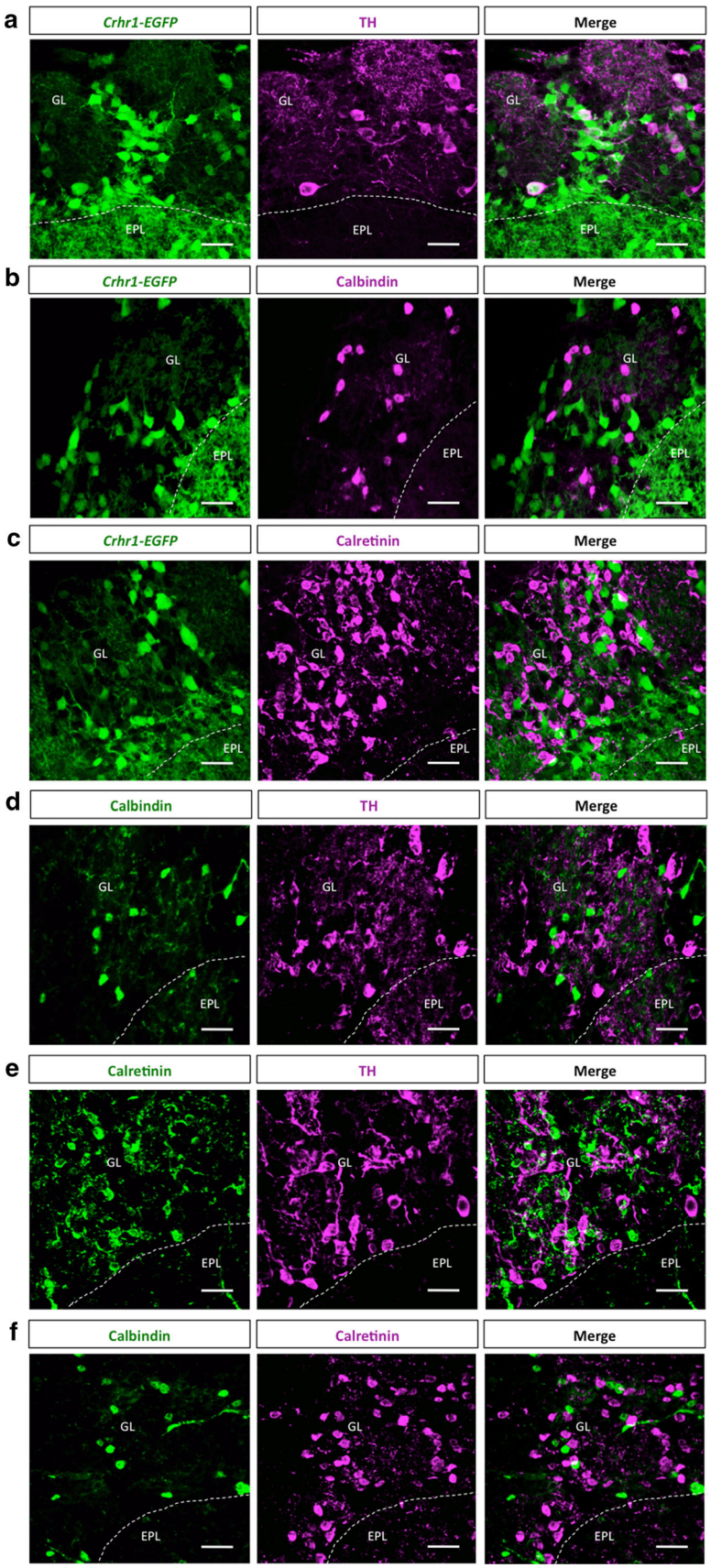

Fig. 6 CRHR1 is expressed by a subset of dopaminergic periglomerular cells. Immunohistochemistry confocal images of *Crhr1-EGFP* olfactory bulb tissue stained with **a** Tyrosine Hydroxylase (TH) (*EPL* external plexiform layer, *GL* glomerular layer, *scale bar* 40 μm), **b** Calbindin (*scale bar* 40 μm), and **c** Calretinin (*scale bar* 40 μm). Confocal images of wild-type olfactory bulb tissue stained with **d** Calbindin and TH (*scale bar* 40 μm), **e** Calretinin and TH (*scale bar* 40 μm), and **f** Calbindin and Calretinin (*scale bar* 40 μm)

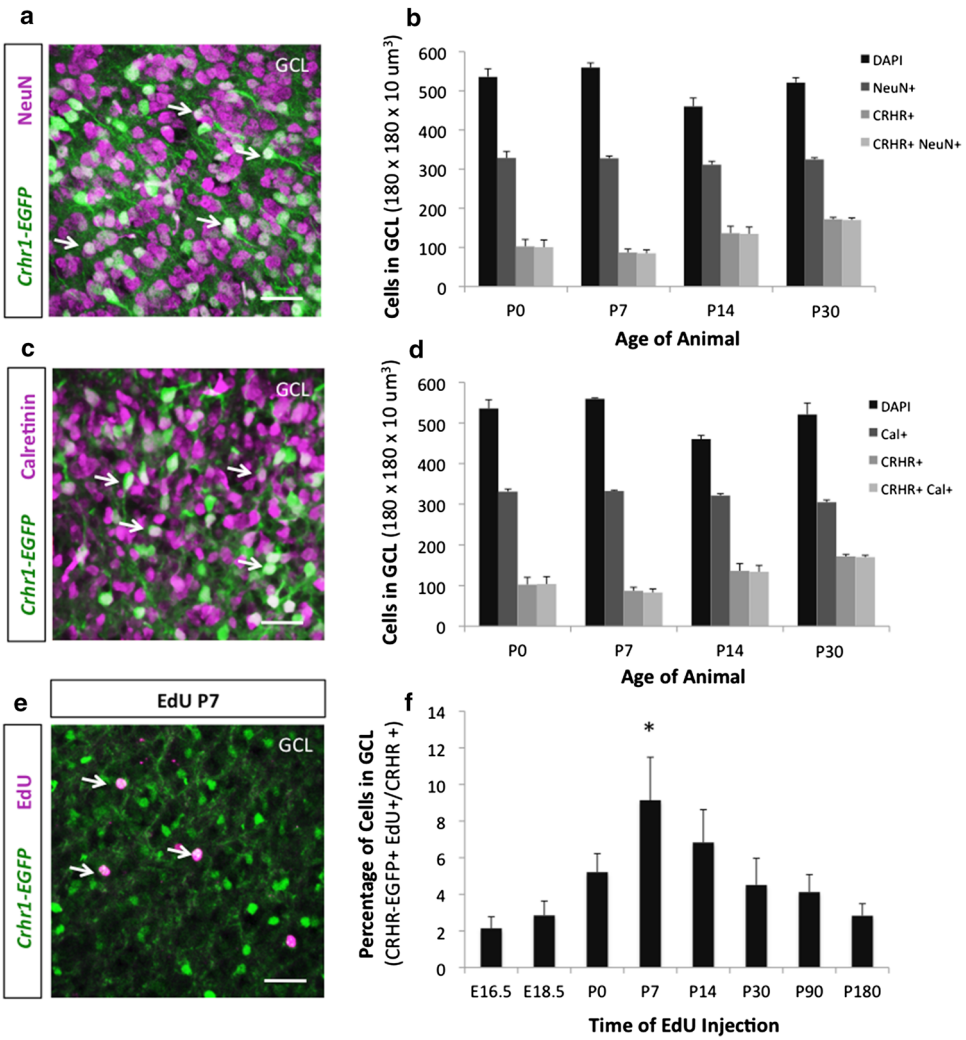

Fig. 7 CRHR1+ granule cells are continuously generated throughout development with postnatal enrichment. **a** Confocal image showing immunodetection of NeuN in the granule cell layer (GCL) of *Crhr1-EGFP* olfactory bulb sections (*scale bar* 30 μm). **b** Quantification of the expression of NeuN and CRHR1+ interneurons in the GCL at P0, P7, P14, and P30. **c** Confocal image showing immunodetection of Calretinin in the GCL of *Crhr1-EGFP* olfactory bulb sections (*scale bar* 30 μm). **d** Quantification of the expression of Calretinin and CRHR1 interneurons in the GCL at P0, P7, P14, and P30. **e** Representative GCL confocal image of EdU-pulsed *Crhr1-EGFP* mice at P7 (*scale bar* 40 μm). **f** Quantification of the percentage of CRHR1+ granule cells born between E16.5 and P180. All data points represent averages ± SEM

synaptic plasticity. Of note, the majority of neurons in the olfactory system have already established their terminal identity by mid-embryonic and early neonatal periods, as suggested by early expression of the neuronal markers NeuN and Calretinin (Fig. 11). In contrast, local CRH expression appears later in the postnatal period, appointing towards a distinct role for neuropeptide signaling between EPL interneurons and CRHR1+ neurons at later developmental stages, and/or throughout adulthood.

Dual roles for neuropeptidergic EPL interneurons

In a previous report, we have characterized CRH+ EPL interneurons as GABAergic, and have functionally shown that they make reciprocal synaptic connections with the principal neurons of the OB (Huang et al. 2013). CRH+ EPL interneurons inhibit mitral/tufted cells via GABA neurotransmission, and are in turn excited by glutamate released from mitral cells. More recently, it has been shown that PV+ EPL interneurons are broadly tuned and influence olfactory circuit function via GABAergic signaling mechanisms (Kato et al. 2013; Miyamichi et al. 2013). Given that this cell population expresses both GABA and the neuropeptide CRH, the question arises if there is a dual functional role for these neurons toward olfactory processing. Our data show that impaired CRH signaling, via removal of CRHR1 from the OB circuitry, leads to abnormal circuit physiology and behavioral responses.

Interestingly, CRHR1+ granule cells vastly outnumber CRH+ EPL interneurons, suggesting that any given EPL interneuron might have an effect on numerous granule cells. Previously, we have shown that EPL interneuron neurites span ~71 μm from the soma (Huang et al. 2013). Given their location within the EPL, this radius is likely to facilitate contacts with numerous granule cell dendrites. Additionally, CRHR1 expression is also found within periglomerular cells. Because we only rarely observed CRH+ terminals directly within the glomerular layer, it is possible that locally secreted CRH diffuses short distances

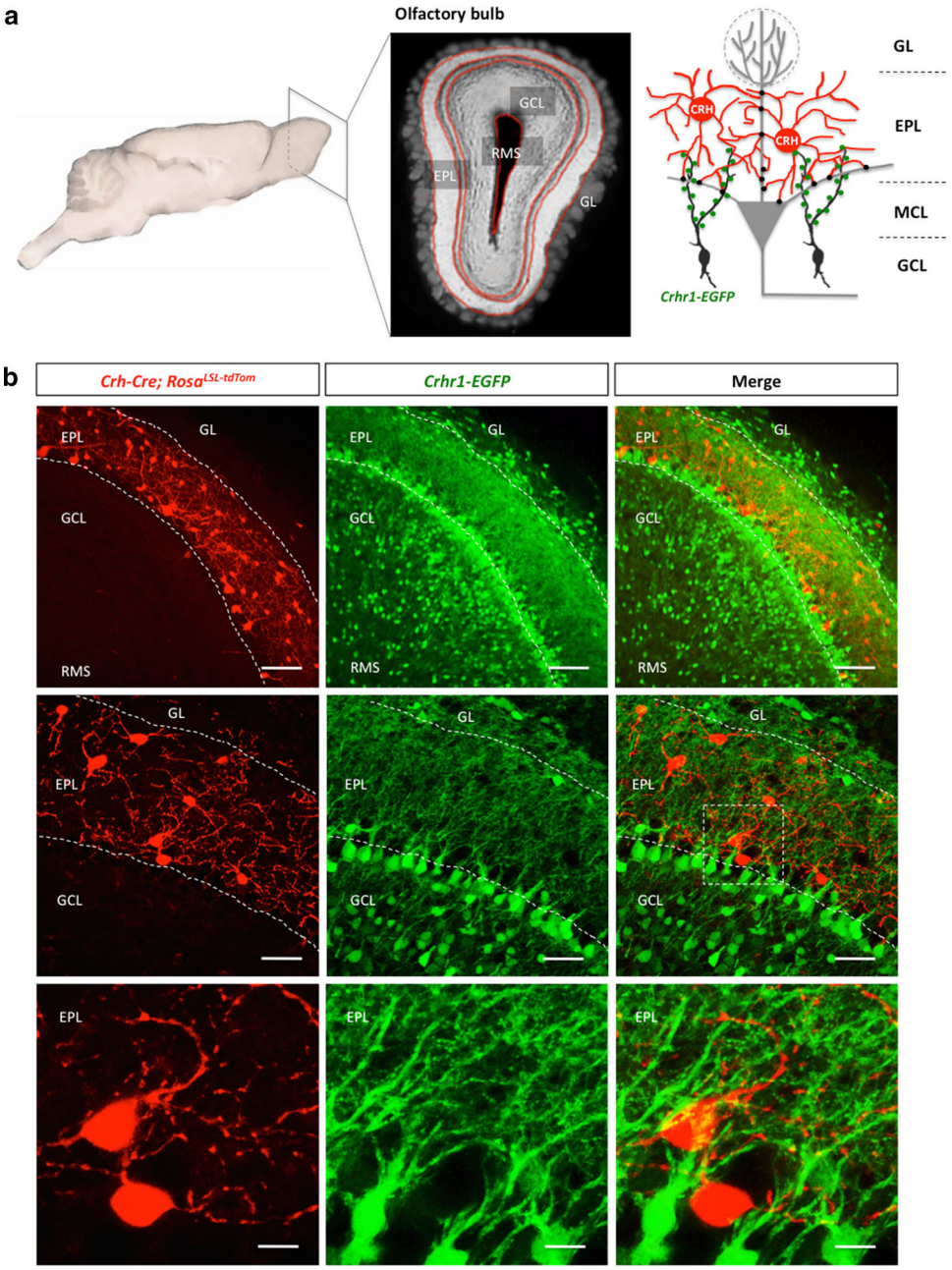

Fig. 8 CRH and CRHR1 expressing interneurons are closely juxtaposed in the mouse olfactory bulb. **a** Simplified schematic of the mouse brain and olfactory bulb circuitry (*GL* glomerular layer, *EPL* external plexiform layer, *MCL* mitral cell layer, *GCL* granule cell layer, *RMS* rostral migratory stream). **b** Confocal images of double-reporter expression in the olfactory bulb of *Crh-Cre*; *Rosa*$^{lsl\text{-}tdTomato/+}$; *Crhr1-EGFP* mice. (*scale bars* 100, 50, and 10 µm, respectively)

to act on periglomerular cells. Together, our data support the idea that neuropeptidergic EPL interneurons have two roles in the OB circuitry, first, to inhibit mitral/tufted cells via GABAergic classical neurotransmission, and second, to act as neuromodulators on granule/periglomerular cells. Because CRHR2 is also present in the OB, it is possible that CRH does not act exclusively via CRHR1, but also via CRHR2. Interestingly, Lovenberg et al. (1995) reported the differential expression pattern of the CRHR2 alpha and beta form, and showed that the alpha form was almost exclusively expressed in the central nervous system and particularly enriched in the hypothalamus, lateral septum, and olfactory bulb. Although CRHR2 is expressed at lower levels than CRHR1 in the OB (Fig. 3a, Allen Brain Atlas, and GENSAT), it is possible that CRH also acts via CRHR2 within the OB. However, the precise downstream signaling mechanism of CRH on CRHR1 and/or CRHR2-expressing cells within the OB remains to be determined.

Local CRH signaling emerges in the postnatal OB

Because the OB is a laminar structure with different functional roles for each layer, the cell type-specific expression of CRH and CRHR1 suggests functional relevance. A previous

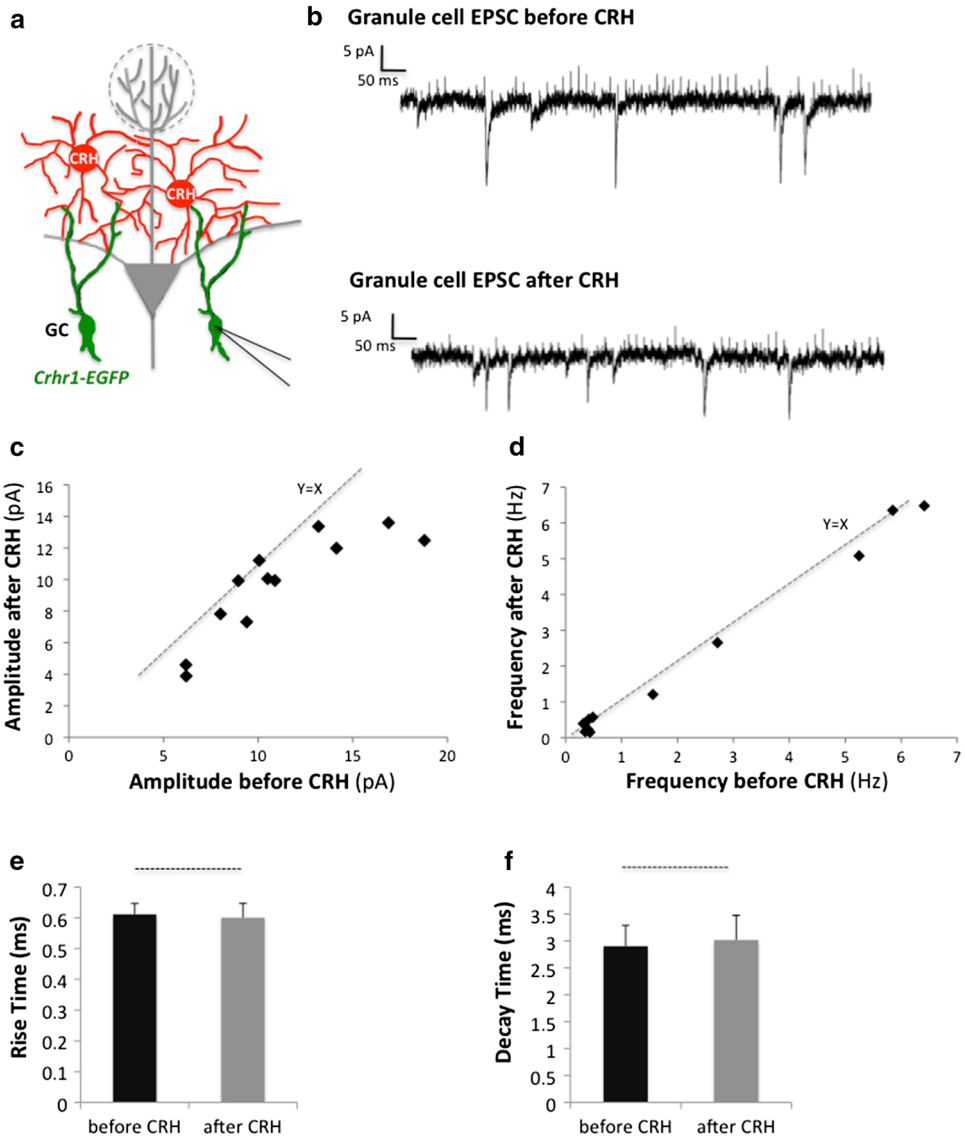

Fig. 9 CRHR1-expressing granule cells show electrophysiological responses to CRH ligand. **a** Experimental scheme: electrophysiological recordings are taken from CRHR1-expressing granule cells via patch clamp before and after bath application of CRH ligand. **b** Representative traces showing EPSCs of recorded granule cells before and after CRH application. **c** Graph of EPSC amplitudes before and after CRH application. **d** Graph of EPSC frequency before and after CRH application. Quantification of the **e** rise time and **f** decay time of granule cell EPSCs. All data points represent mean ± SEM ($n = 12$ cells per group from 3 mice)

report (Batista-Brito et al. 2008) has shown that different OB interneuron subtypes are produced during distinct developmental stages. For example, PV+ EPL interneurons are predominantly generated in the postnatal period, suggesting that EPL interneurons might become physiologically relevant postnatally. Interestingly, EPL interneuron-mitral/tufted cell synapses are also formed postnatally. It remains to be determined in future studies if these cell connections are stable or plastic throughout the animal's life. In contrast, granule cells are continuously generated throughout life. Thus, EPL interneuron connections onto granule cells are either highly plastic, in that they continuously form connections onto newly generated CRHR1+ granule cells, or that CRH+ EPL interneuron connections might be stable and it is the diffusion of secreted CRH that acts onto CRHR1+ cells via an extrasynaptic mechanism.

Interestingly, we found that there appear to be two different waves of CRHR1+ granule cells that populate the OB. Whereas CRHR expression is enriched in the outer granule cell and mitral layers between postnatal days 7–14, the inner granule cell layer becomes populated with CRHR+ cells between postnatal days 14–30, and remains stable thereafter (Fig. 4). Intriguingly, the first wave of CRHR1+ granule cells is coincident with the appearance of CRH+ EPL interneurons during the postnatal period (Figs. 1, 2). This differential pattern of developmental expression suggests that there may be distinct signaling mechanisms that guide early postnatal and adult neurogenesis. Recent studies discovered that a Foxj1-dependent lineage in the forebrain is required for the overall postnatal neurogenesis in the OB (Jacquet et al. 2011; Muthusamy et al. 2014), that Foxj1-derived neurons arrived in the OB

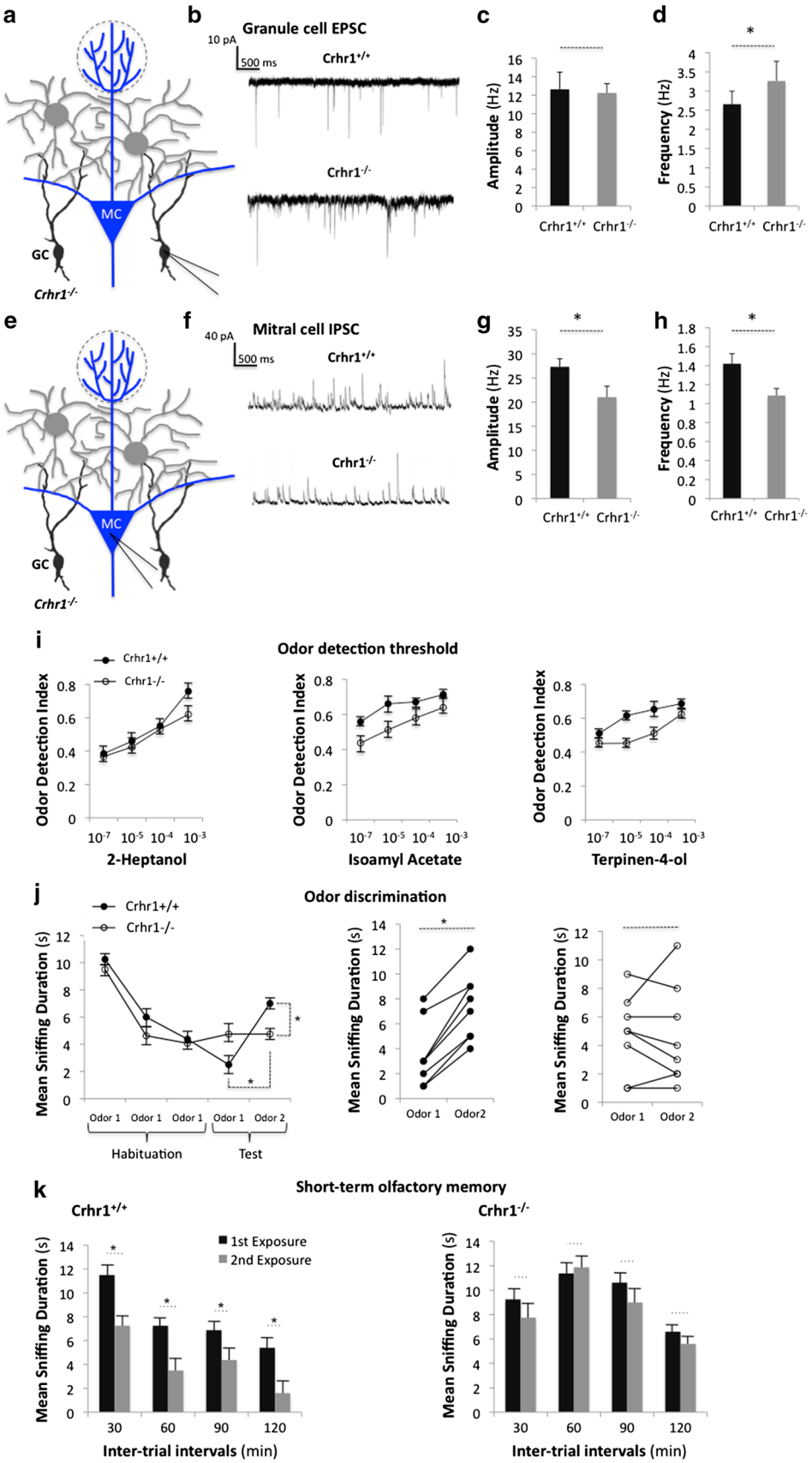

Fig. 10 Mice lacking CRHR1 show olfactory bulb circuit dysfunction and impaired olfactory behaviors. **a** Experimental scheme: electrophysiological recordings are taken from granule cells in $Crhr1^{-/-}$ slices via patch clamp. **b** Representative traces showing EPSCs from $Crhr1^{+/+}$ and $Crhr1^{-/-}$ granule cells. Quantification of the **c** amplitudes and **d** frequencies of granule cell EPSCs ($*p < 0.05$, $n = 10$ cells per group from 3 mice). **e** Experimental scheme: electrophysiological recordings are taken from mitral cells in $Crhr1^{-/-}$ olfactory bulb slices. **f** Representative traces showing IPSCs from mitral cells of $Crhr1^{+/+}$ and $Crhr1^{-/-}$ olfactory bulbs. Quantification of the **g** amplitudes and **h** frequencies of mitral cell IPSCs ($*p < 0.05$, $n = 10$ cells per group from 3 mice). **i** Odor detection threshold of control and $Crhr1^{-/-}$ mice at concentrations from 10^{-7} to 10^{-3}. **j** Odor discrimination and **k** short-term olfactory memory performance of $Crhr1^{-/-}$ mice compared to controls ($*p < 0.05$). All behavior data points represent mean ± SEM, $n = 8$ animals per group

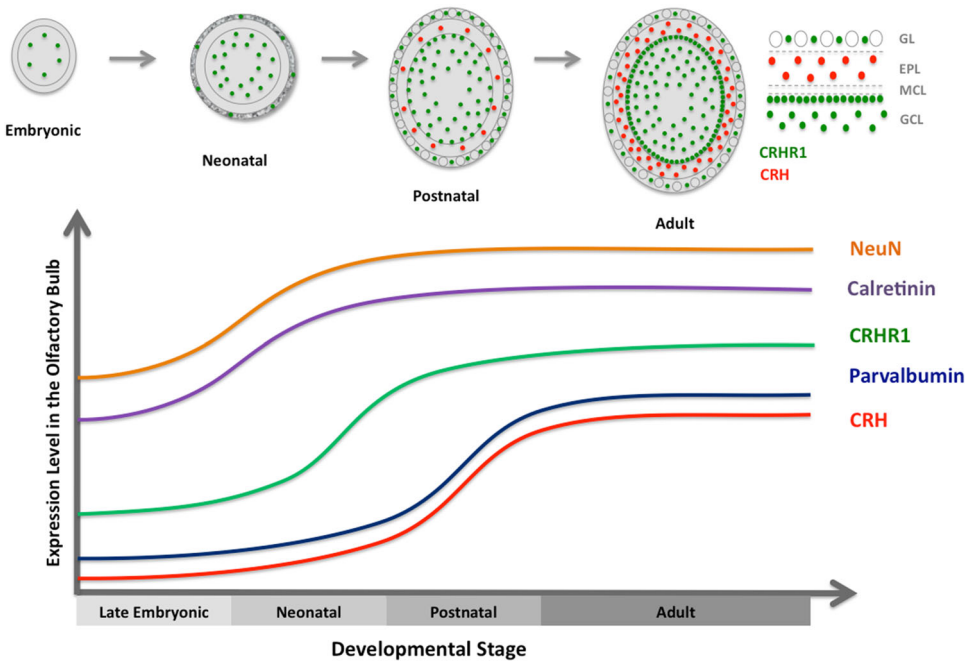

Fig. 11 CRH and CRHR1 expression in the olfactory bulb become enriched in the postnatal period. During development, olfactory bulb CRHR1 expression appears first in the embryonic period and then gradually increases to reach a steady state in adulthood. CRH expression turns on postnatally and increases into early adulthood, remaining stable thereafter

between P0 and P21, and that these unique cells populated both the mitral cell and granule cell layers, and persist during adulthood (Jacquet et al. 2011). Furthermore, Foxj1-derived neurons affect postnatal and adult neurogenesis in a paracrine manner. Interestingly, although Foxj1-derived neurons in the OB only make up ~3 % of the total cell number, *Foxj1*$^{-/-}$ mice show a 65 % reduction in the total population of neurons in the OB (Jacquet et al. 2011). Moreover, the identity of Foxj1-derived neurons still remains in question, since they did express known granule cell markers. Given our data, it is possible that this distinct cell population consists of the postnatal wave of neurons we have identified to be CRH and CRHR1+, which remains to be determined.

It is likely no coincidence that the expression of CRH and CRHR1 in the OB occurs in a paired manner, and supports a physiological role for neuropeptide signaling onto granule and/or periglomerular cells. This is particularly interesting since granule cells undergo continuous regeneration in the OB, and that their survival and function is dynamically regulated via levels of neuronal activity (Abrous et al. 2005; Ming and Song 2005). Also, given that *Crhr1*$^{-/-}$ mice show abnormal electrophysiology, odor discrimination, and olfactory memory performance, it is possible that CRH signaling is a key mediator of activity within the OB circuitry. However, it is important to interpret these results with caution since we cannot rule out combinatorial effects on olfactory processes with loss of other brain region-specific CRH signaling mechanisms potentially contributing to abnormal olfactory behaviors in these mice.

The role of CRH on olfactory learning processes

Given that CRH has traditionally been studied as a signaling molecule released in times of stress, the question arises if the increased stress levels cause modulation and/or release of CRH by EPL interneurons within the OB. Other studies have demonstrated that CRH is released from neurons in different regions of the brain during stress. For example, CRH has been found in the developing and adult hippocampus (Sakanaka et al. 1987; Chen et al. 2001, 2012), amygdala (Roozendaal et al. 2002), and locus coeruleus (Valentino and Wehby 1988; Snyder et al. 2012). Interestingly, it has been discovered that early life stress disrupts maternal attachment learning and increases aversion learning via a unique pathway in which corticosteroids released during stress activate the amygdala, which in turn excite the locus coeruleus via CRH afferents and increases norepinephrine levels within the OB (Moriceau et al. 2009). The precise role of local OB CRH release during stress responses remains unknown. However, our data suggest that CRH acts as a neuromodulator within the OB to shape physiological outputs and olfactory-related learning processes.

Finally, it is intriguing that in addition to CRH, the OB contains an abundance of other local neuropeptides, including somatostatin, vasoactive intestinal peptide, cholecystokinin, neuropeptide Y, and oxytocin (Gracia-Llanes et al. 2003; Lepousez et al. 2010a, b; Ma et al. 2013; Tobin et al. 2010). This suggests the presence of the different neuropeptide receptors within the different cell populations of the OB. It remains to be determined if these locally

secreted neuropeptides all act via distinct mechanisms, or in a redundant manner to allow for the proper functioning of the olfactory system.

Acknowledgments We would like to thank Dr. Roy Sillitoe for critical comments on this manuscript. This work was supported through the McNair Medical Institute, and NINDS awards 1F31NS081805 to I.G. and 1R01NS078294 to B.R.A. The project described was supported in part by the RNA in situ Hybridization Core facility at Baylor College of Medicine, which is supported by a shared instrumentation Grant from the NIH (1S10OD016167) and the NIH IDDRC Grant 5P30HD024064 from the Eunice Kennedy Shriver National Institute of Child Health and Human Development.

References

Abraham NM, Egger V, Shimshek DR, Renden R, Fukunaga I, Sprengel R, Seeburg PH, Klugmann M, Margrie TW, Schaefer AT et al (2010) Synaptic inhibition in the olfactory bulb accelerates odor discrimination in mice. Neuron 65:399–411

Abrous DN, Koehl M, Le Moal M (2005) Adult neurogenesis: from precursors to network and physiology. Physiol Rev 85:523–569

Alvarez-Buylla A, Garcia-Verdugo JM (2002) Neurogenesis in adult subventricular zone. J Neurosci 22:629–634

Arenkiel BR, Hasegawa H, Yi JJ, Larsen RS, Wallace ML, Philpot BD, Wang F, Ehlers MD (2011) Activity-induced remodeling of olfactory bulb microcircuits revealed by monosynaptic tracing. PLoS One 6:e29423

Bale TL, Vale WW (2004) CRF and CRF receptors: role in stress responsivity and other behaviors. Annu Rev Pharmacol Toxicol 44:525–557

Batista-Brito R, Close J, Machold R, Fishell G (2008) The distinct temporal origins of olfactory bulb interneuron subtypes. J Neurosci 28:3966–3975

Bayatti N, Zschocke J, Behl C (2003) Brain region-specific neuroprotective action and signaling of corticotropin-releasing hormone in primary neurons. Endocrinology 144:4051–4060

Belnoue L, Grosjean N, Abrous DN, Koehl M (2011) A critical time window for the recruitment of bulbar newborn neurons by olfactory discrimination learning. J Neurosci 31:1010–1016

Berger H, Heinrich N, Wietfeld D, Bienert M, Beyermann M (2006) Evidence that corticotropin-releasing factor receptor type 1 couples to Gs- and Gi-proteins through different conformations of its J-domain. Br J Pharmacol 149:942–947

Blank T, Nijholt I, Grammatopoulos DK, Randeva HS, Hillhouse EW, Spiess J (2003) Corticotropin-releasing factor receptors couple to multiple G-proteins to activate diverse intracellular signaling pathways in mouse hippocampus: role in neuronal excitability and associative learning. J Neurosci 23:700–707

Breton-Provencher V, Lemasson M, Peralta MR 3rd, Saghatelyan A (2009) Interneurons produced in adulthood are required for the normal functioning of the olfactory bulb network and for the execution of selected olfactory behaviors. J Neurosci 29:15245–15257

Chaves VE, Tilelli CQ, Brito NA, Brito MN (2013) Role of oxytocin in energy metabolism. Peptides 45:9–14

Chen WR, Xiong W, Shepherd GM (2000) Analysis of relations between NMDA receptors and GABA release at olfactory bulb reciprocal synapses. Neuron 25:625–633

Chen Y, Bender RA, Frotscher M, Baram TZ (2001) Novel and transient populations of corticotropin-releasing hormone-expressing neurons in developing hippocampus suggest unique functional roles: a quantitative spatiotemporal analysis. J Neurosci 21:7171–7181

Chen Y, Bender RA, Brunson KL, Pomper JK, Grigoriadis DE, Wurst W, Baram TZ (2004) Modulation of dendritic differentiation by corticotropin-releasing factor in the developing hippocampus. Proc Natl Acad Sci USA 101:15782–15787

Chen J, Evans AN, Liu Y, Honda M, Saavedra JM, Aguilera G (2012) Maternal deprivation in rats is associated with corticotrophin-releasing hormone (CRH) promoter hypomethylation and enhances CRH transcriptional responses to stress in adulthood. J Neuroendocrinol 24:1055–1064

Eyre MD, Antal M, Nusser Z (2008) Distinct deep short-axon cell subtypes of the main olfactory bulb provide novel intrabulbar and extrabulbar GABAergic connections. J Neurosci 28:8217–8229

Gheusi G, Cremer H, McLean H, Chazal G, Vincent JD, Lledo PM (2000) Importance of newly generated neurons in the adult olfactory bulb for odor discrimination. Proc Natl Acad Sci USA 97:1823–1828

Gheusi G, Lepousez G, Lledo PM (2013) Adult-born neurons in the olfactory bulb: integration and functional consequences. Curr Top Behav Neurosci 2013(15):49–72

Gracia-Llanes FJ, Crespo C, Blasco-Ibanez JM, Marques-Mari AI, Martinez-Guijarro FJ (2003) VIP-containing deep short-axon cells of the olfactory bulb innervate interneurons different from granule cells. Eur J Neurosci 18:1751–1763

Hamilton KA, Heinbockel T, Ennis M, Szabo G, Erdelyi F, Hayar A (2005) Properties of external plexiform layer interneurons in mouse olfactory bulb slices. Neuroscience 133(3):819–829

Hanstein R, Lu A, Wurst W, Holsboer F, Deussing JM, Clement AB, Behl C (2008) Transgenic overexpression of corticotropin releasing hormone provides partial protection against neurodegeneration in an in vivo model of acute excitotoxic stress. Neuroscience 156:712–721

Holzer P, Reichmann F, Farzi A (2012) Neuropeptide Y, peptide YY and pancreatic polypeptide in the gut-brain axis. Neuropeptides 46:261–274

Huang L, Garcia I, Jen HI, Arenkiel BR (2013) Reciprocal connectivity between mitral cells and external plexiform layer interneurons in the mouse olfactory bulb. Front Neural Circuits 7:32

Inutsuka A, Yamanaka A (2013a) The physiological role of orexin/hypocretin neurons in the regulation of sleep/wakefulness and neuroendocrine functions. Front Endocrinol (Lausanne) 4:18

Inutsuka A, Yamanaka A (2013b) The regulation of sleep and wakefulness by the hypothalamic neuropeptide orexin/hypocretin. Nagoya J Med Sci 75:29–36

Iovino M, Guastamacchia E, Giagulli VA, Licchelli B, Triggiani V (2012) Vasopressin secretion control: central neural pathways, neurotransmitters and effects of drugs. Curr Pharm Des 18:4714–4724

Isaacson JS, Strowbridge BW (1998) Olfactory reciprocal synapses: dendritic signaling in the CNS. Neuron 20:749–761

Jacquet BV, Muthusamy N, Sommerville LJ, Xiao G, Liang H, Zhang Y, Holtzman MJ, Ghashghaei HT (2011) Specification of a Foxj1-dependent lineage in the forebrain is required for embryonic-to-postnatal transition of neurogenesis in the olfactory bulb. J Neurosci 31(25):9368–9382

Justice NJ, Yuan ZF, Sawchenko PE, Vale W (2008) Type 1 corticotropin-releasing factor receptor expression reported in BAC transgenic mice: implications for reconciling ligand-receptor mismatch in the central corticotropin-releasing factor system. J Comp Neurol 511:479–496

Kato HK, Gillet SN, Peters AJ, Isaacson JS, Komiyama T (2013) Parvalbumin-expressing interneurons linearly control olfactory bulb output. Neuron 80:1218–1231

Kelsch W, Lin CW, Mosley CP, Lois C (2009) A critical period for activity-dependent synaptic development during olfactory bulb adult neurogenesis. J Neurosci 29:11852–11858

Kosaka T, Kosaka K (2008) Heterogeneity of parvalbumin-containing neurons in the mouse main olfactory bulb, with special reference to short-axon cells and betaIV-spectrin positive dendritic segments. Neurosci Res 60:56–72

Lazarini F, Mouthon MA, Gheusi G, de Chaumont F, Olivo-Marin JC, Lamarque S, Abrous DN, Boussin FD, Lledo PM (2009) Cellular and behavioral effects of cranial irradiation of the subventricular zone in adult mice. PLoS One 4:e7017

Le Magueresse C, Monyer H (2013) GABAergic interneurons shape the functional maturation of the cortex. Neuron 77:388–405

Lepousez G, Csaba Z, Bernard V, Loudes C, Videau C, Lacombe J, Epelbaum J, Viollet C (2010a) Somatostatin interneurons delineate the inner part of the external plexiform layer in the mouse main olfactory bulb. J Comp Neurol 518: 1976–1994

Lepousez G, Mouret A, Loudes C, Epelbaum J, Viollet C (2010b) Somatostatin contributes to in vivo gamma oscillation modulation and odor discrimination in the olfactory bulb. J Neurosci 30:870–875

Lledo PM, Saghatelyan A (2005) Integrating new neurons into the adult olfactory bulb: joining the network, life death decisions, and the effects of sensory experience. Trends Neurosci 28:248–254

Lovenberg TW, Chalmers DT, Liu C, De Souza EB (1995) CRF2 alpha and CRF2 beta receptor mRNAs are differentially distributed between the rat central nervous system and peripheral tissues. Endocrinology 136(9):4139–4142

Luo M, Katz LC (2001) Response correlation maps of neurons in the mammalian olfactory bulb. Neuron 32:1165–1179

Ma Y, Hu H, Berrebi AS, Mathers PH, Agmon A (2006) Distinct subtypes of somatostatin-containing neocortical interneurons revealed in transgenic mice. J Neurosci 26:5069–5082

Ma S, Blasiak A, Olucha-Bordonau FE, Verberne AJ, Gundlach AL (2013) Heterogeneous responses of nucleus incertus neurons to corticotropin-releasing factor and coherent activity with hippocampal theta rhythm in the rat. J Physiol 591:3981

Maras PM, Baram TZ (2012) Sculpting the hippocampus from within: stress, spines, and CRH. Trends Neurosci 35:315–324

Merrill L, Girard B, Arms L, Guertin P, Vizzard MA (2013) Neuropeptide/receptor expression and plasticity in micturition pathways. Curr Pharm Des 19:4411–4422

Ming GL, Song H (2005) Adult neurogenesis in the mammalian central nervous system. Annu Rev Neurosci 28:223–250

Ming GL, Song H (2011) Adult neurogenesis in the mammalian brain: significant answers and significant questions. Neuron 70(4):687–702

Mitsui S, Igarashi KM, Mori K, Yoshihara Y (2011) Genetic visualization of the secondary olfactory pathway in Tbx21 transgenic mice. Neural Syst Circuits 1(1):5

Miyamichi K, Shlomai-Fuchs Y, Shu M, Weissbourd BC, Luo L, Mizrahi A (2013) Dissecting local circuits: parvalbumin interneurons underlie broad feedback control of olfactory bulb output. Neuron 80:1232–1245

Moriceau S, Shionoya K, Jakubs K, Sullivan RM (2009) Early-life stress disrupts attachment learning: the role of amygdala corticosterone, locus ceruleus corticotropin releasing hormone, and olfactory bulb norepinephrine. J Neurosci 29(50):15745–15755

Mouret A, Lepousez G, Gras J, Gabellec MM, Lledo PM (2009) Turnover of newborn olfactory bulb neurons optimizes olfaction. J Neurosci 29:12302–12314

Mullen RJ, Buck CR, Smith AM (1992) NeuN, a neuronal specific nuclear protein in vertebrates. Development 116:201–211

Muthusamy N, Vijayakumar A, Cheng JG, Ghashghaei HT (2014) A knock-in Foxj1$^{CreERT2:GFP}$ mouse for recombination in epithelial cells with motile cilia. Genesis 52:350–358

Perrin MH, Donaldson CJ, Chen R, Lewis KA, Vale WW (1993) Cloning and functional expression of a rat brain corticotropin releasing factor (CRF) receptor. Endocrinology 133:3058–3061

Perrin M, Donaldson C, Chen R, Blount A, Berggren T, Bilezikjian L, Sawchenko P, Vale W (1995) Identification of a second corticotropin-releasing factor receptor gene and characterization of a cDNA expressed in heart. Proc Natl Acad Sci USA 92:2969–2973

Pressler RT, Strowbridge BW (2006) Blanes cells mediate persistent feedforward inhibition onto granule cells in the olfactory bulb. Neuron 49:889–904

Ramirez-Sanchez M, Prieto I, Wangensteen R, Banegas I, Segarra AB, Villarejo AB, Vives F, Cobo J, de Gasparo M (2013) The renin-angiotensin system: new insight into old therapies. Curr Med Chem 20:1313–1322

Rochefort C, Gheusi G, Vincent JD, Lledo PM (2002) Enriched odor exposure increases the number of newborn neurons in the adult olfactory bulb and improves odor memory. J Neurosci 22:2679–2689

Roozendaal B, Brunson KL, Holloway BL, McGaugh JL, Baram TZ (2002) Involvement of stress-released corticotropin-releasing hormone in the basolateral amygdala in regulating memory consolidation. Proc Natl Acac Sci USA 99:13908–13913

Rudy B, Fishell G, Lee S, Hjerling-Leffler J (2011) Three groups of interneurons account for nearly 100% of neocortical GABAergic neurons. Dev Neurobiol 71:45–61

Sakanaka M, Shibasaki T, Lederis K (1987) Corticotropin releasing factor-like immunoreactivity in the rat brain as revealed by modified cobalt-glucose-oxidase-diaminobenzidine method. J Comp Neurol 260:256–298

Schmolesky MT, De Ruiter MM, De Zeeuw CI, Hansel C (2007) The neuropeptide corticotropin-releasing factor regulates excitatory transmission and plasticity at the climbing fibre-purkinje cell synapse. Eur J Neurosci 25(5):1460–1467

Schoppa NE, Kinzie JM, Sahara Y, Segerson TP, Westbrook GL (1998) Dendrodendritic inhibition in the olfactory bulb is driven by NMDA receptors. J Neurosci 18:6790–6802

Selever J, Kong JQ, Arenkiel BR (2011) A rapid approach to high-resolution fluorescence imaging in semi-thick brain slices. J Vis Exp

Sheng H, Xu Y, Chen Y, Zhang Y, Ni X (2012) Corticotropin-releasing hormone stimulates mitotic kinesin-like protein 1 expression via a PLC/PKC-dependent signaling pathway in hippocampal neurons. Mol Cell Endocrinol 362:157–164

Smith GW, Aubry JM, Dellu F, Contarino A, Bilezikjian LM, Gold LH, Chen R, Marchuk Y, Hauser C, Bentley CA et al (1998) Corticotropin releasing factor receptor 1-deficient mice display decreased anxiety, impaired stress response, and aberrant neuroendocrine development. Neuron 20:1093–1102

Snyder K, Wang WW, Han R, McFadden K, Valentino RJ (2012) Corticotropin-releasing factor in the norepinephrine nucleus, locus coeruleus, facilitates behavioral flexibility. Neuropsychopharmacology 37:520–530

Taniguchi H, He M, Wu P, Kim S, Paik R, Sugino K, Kvitsiani D, Fu Y, Lu J, Lin Y et al (2011) A resource of Cre driver lines for genetic targeting of GABAergic neurons in cerebral cortex. Neuron 71:995–1013

Thiel G, Cibelli G (1999) Corticotropin-releasing factor and vasoactive intestinal polypeptide activate gene transcription through the cAMP signaling pathway in a catecholaminergic immortalized neuron. Neurochem Int 34:183–191

Tobin VA, Hashimoto H, Wacker DW, Takayanagi Y, Langnaese K, Caquineau C, Noack J, Landgraf R, Onaka T, Leng G et al

(2010) An intrinsic vasopressin system in the olfactory bulb is involved in social recognition. Nature 464:413–417

Vale W, Spiess J, Rivier C, Rivier J (1981) Characterization of a 41-residue ovine hypothalamic peptide that stimulates secretion of corticotropin and beta-endorphin. Science 213:1394–1397

Vale W, Rivier C, Brown MR, Spiess J, Koob G, Swanson L, Bilezikjian L, Bloom F, Rivier J (1983) Chemical and biological characterization of corticotropin releasing factor. Recent Prog Horm Res 39:245–270

Valentino RJ, Wehby RG (1988) Corticotropin-releasing factor: evidence for a neurotransmitter role in the locus coeruleus during hemodynamic stress. Neuroendocrinology 48:674–677

Xu H, Jeong HY, Tremblay R, Rudy B (2013) Neocortical somatostatin-expressing GABAergic interneurons disinhibit the thalamorecipient layer 4. Neuron 77:155–167

Yamaguchi M, Mori K (2005) Critical period for sensory experience-dependent survival of newly generated granule cells in the adult mouse olfactory bulb. Proc Natl Acad Sci USA 102:9697–9702

Yaylaoglu MB, Titmus A, Visel A, Alvarez-Bolado G, Thaller C, Eichele G (2005) Comprehensive expression atlas of fibroblast growth factors and their receptors generated by a novel robotic in situ hybridization platform. Dev Dyn 234:371–386

Zwanzger P, Domschke K, Bradwejn J (2012) Neuronal network of panic disorder: the role of the neuropeptide cholecystokinin. Depress Anxiety 29:762–774